World Applied Sciences Journal 23 (8): 998-1006, 2013
ISSN 1818-4952

DOI: 10.5829/idosi.wasj.2013.23.08.1762

Stagnation-Point Flow of a Nanofluid Over a Nonlinear Stretching Sheet

[1,2]M.I. Anwar, [1]I. Khan, [1]A. Hussanan, [3]M.Z. Salleh and [1]S. Sharidan
[1]Department of Mathematical Sciences, Faculty of Science,
Universiti Teknologi Malaysia, UTM 81310 Skudai, Johor, Malaysia
[2]Department of Mathematics, Faculty of Science, University of Sargodha, Pakistan.
[3]Faculty of Industrial Science and Technology, Universiti Malaysia Pahang,
UMP 26300 Kuantan, Pahang, Malaysia

Submitted: May 15, 2013; **Accepted:** Jun 23, 2013; **Published:** Jul 22, 2013

Abstract: Stagnation-point flow of a nanofluid over a nonlinear stretching sheet is investigated theoretically when the sheet is stretched with a power law velocity under a constant wall temperature. The governing nonlinear problem incorporates the effects of Brownian motion and thermophoresis is transformed by using appropriate similarity transformations into ordinary differential equations. These equations along with boundary conditions are solved numerically by using implicit finite difference scheme known as the Keller-box method. The obtained numerical results are plotted graphically for the interesting flow parameters. The results of Khan and Pop [6] are reduced as the limiting cases of the present studies.

Key words: Nanofluid · Stagnation-point flow · Nonlinear stretching sheet · Numerical solution

INTRODUCTION

The interest of researchers in nanofluid increases rapidly due to its several industrial, engineering and technological applications such as chemical catalytic reactors, grain storage installations, diffusion of medicine in blood veins and cooling of electronic equipment. However, due to the additional nonlinear terms in the equation of motion make it more complex that's why a limited attention was given to these fluids. There are some important recent studies of nanofluid introduced in the literature [1-7]. Choi [8] introduced convection heat transfer fluids as nanofluid having substantially higher thermal conductivities to study the enhancement in heat transfer phenomenon. Furthermore, some important experimental studies have been done [9-11] to evaluate the increase in the thermal conductivities of nanofluid.

On the other hand, a stagnation-point occurs whenever a flow impinges on a solid object. For orthogonally or non-orthogonally/obliquely stagnated flows, the velocities go to zero along with the highest pressure on the surface [12]. Based on the pioneering work of Heimenz [13], many researchers have discussed the stagnation point flows on stretching sheet [14-16]. Mustafa *et al*. [17] studied the stagnation-point flow of a nanofluid towards a stretching sheet. Hamad and Ferdows [18] presented a Lie group analysis to find the similarity solution of boundary layer stagnation-point flow towards a heated porous stretching sheet saturated with a nanofluid with heat absorption/generation and suction/ blowing. After words, Alsaedi *et al*. [19] obtained results for convective boundaries by considering the effects of heat generation/absorption on stagnation-point flow.

To the best of our knowledge, no attention has been focused on stagnation-point flow of nanofluid over a nonlinear stretching sheet. Hence this motivates us to make such an attempt. The governing equations are modeled and numerically solved using an implicit finite difference scheme known as Keller-box method.

Problem Formulation: A steady two-dimensional boundary layer stagnation-point flow of a nanofluid over a nonlinear stretching sheet is considered. The stretching and free stream velocities are assumed of the forms $u_w(x) = ax^m$ and $u_\infty(x) = bx^m$ respectively, where a, b are constant parameters, m ($m \geq 0$) is the velocity exponent parameter and x is the coordinate measured along the stretching surface. It is assumed that at the stretching

Corresponding Author: S. Sharidan, Department of Mathematical Sciences, Faculty of Science,
Universiti Teknologi Malaysia, UTM 81310 Skudai, Johor, Malaysia.
Tel: +6-013-7731773, Fax: +6-07-5566162.

surface, the temperature T and the nanoparticles fraction C take constant values T_w and C_w whereas the ambient values of temperature T_∞ and the nanoparticles fraction C_∞ are attained as y tends to infinity. The governing boundary layer equations for momentum, energy and concentration are given as follows [4, 6, 7].

$$\frac{\partial u}{\partial x}+\frac{\partial v}{\partial y}=0, \tag{1}$$

$$\frac{\partial p}{\partial x}=\mu\frac{\partial^2 u}{\partial y^2}-\rho_f\left(u\frac{\partial u}{\partial x}+v\frac{\partial u}{\partial y}\right), \tag{2}$$

$$u\frac{\partial T}{\partial x}+v\frac{\partial T}{\partial y}=\alpha\frac{\partial^2 T}{\partial y^2}+\tau\left[D_B\frac{\partial C}{\partial y}\frac{\partial T}{\partial y}+\frac{D_T}{T_\infty}\left(\frac{\partial T}{\partial y}\right)^2\right], \tag{3}$$

$$u\frac{\partial C}{\partial x}+v\frac{\partial C}{\partial y}=D_B\frac{\partial^2 C}{\partial y^2}+\frac{D_T}{T_\infty}\frac{\partial^2 T}{\partial y^2}, \tag{4}$$

where u and v are the velocity components in the x and y – directions respectively, μ is the viscosity, ρ_f is the density of the base fluid, D_B is the Brownian diffusion coefficient, D_T is the thermophoresis diffusion coefficient, $\alpha = k/(\rho c)_f$ where k is the thermal conductivity and $(\rho c)_f$ is the heat capacitance of the base fluid, $\tau = (\rho c)_p/(pc)_f$ where $(pc)_p$ is the heat capacitance of the nanoparticles. The associated boundary conditions are:

$$\begin{aligned}&u=u_w(x)=ax^m,\ v=0,\ T=T_w,\ C=C_w \text{ at } y=0,\\ &u\to u_\infty(x)=bx^m,\ v\to 0,\ T\to T_\infty,\ C\to C_\infty \text{ as } y\to\infty.\end{aligned} \tag{5}$$

Using the stream function $\psi = \psi(x, y)$ the continuity Eq. (1) is satisfied identically for the velocity components u and v defined as:

$$u=\frac{\partial\psi}{\partial y},\ v=-\frac{\partial\psi}{\partial x}. \tag{6}$$

Following Afify [20], similarity transformations are defined as follows:

$$\begin{aligned}&\psi=\sqrt{\frac{2\nu a x^{m+1}}{m+1}}f(\eta),\ \theta(\eta)=\frac{T-T_\infty}{T_w-T_\infty},\\ &\phi(\eta)=\frac{C-C_\infty}{C_w-C_\infty},\ \eta=y\sqrt{\frac{(m+1)ax^{m-1}}{2\nu}}.\end{aligned} \tag{7}$$

On using Eq. (7) into Eqs. (2)-(4), we get the coupled system of ordinary differential equations,

$$f'''+ff''-\left(\frac{2m}{m+1}\right)f'^2+\left(\frac{2m}{m+1}\right)\varepsilon^2=0, \tag{8}$$

$$\frac{1}{\Pr}\theta''+f\theta'+Nb\phi'\theta'+Nt\theta'^2=0, \tag{9}$$

$$\phi''+Lef\phi'+\frac{Nt}{Nb}\theta''=0, \tag{10}$$

where

$$\varepsilon=\frac{b}{a},\ \Pr=\frac{\nu}{\alpha},\ Le=\frac{\nu}{D_B},\ \nu=\frac{\mu}{\rho_f},\ Nb=\frac{\tau D_B(C_w-C_\infty)}{\nu},\ Nt=\frac{\tau D_T(T_w-T_\infty)}{\nu T_\infty}.$$

Here ε is the velocity ratio parameter, Pr is the Prandtl number, Le is the Lewis number, ν is the kinematic viscosity of the fluid, Nb is the Brownian motion parameter, Nt is the thermophoresis parameter, f, θ and ϕ are the dimensionless stream function, temperature and rescaled nanoparticles volume fraction respectively.

The corresponding boundary conditions are transformed to:

$$\begin{aligned}&f=0,\ f'=1,\ \theta=1,\ \phi=1 \quad \text{at} \quad \eta=0,\\ &f'\to\varepsilon,\ \theta\to 0,\ \phi\to 0 \quad \text{as} \quad \eta\to\infty.\end{aligned} \tag{11}$$

The Nusselt number, Sherwood number and skin-friction for the present problem of nanofluid are defined as:

$$Nu=\frac{q_w x}{k(T_w-T_\infty)},\ Sh=\frac{q_m x}{k(C_w-C_\infty)},\ C_f=\frac{\tau_w}{\frac{1}{2}\rho U^2},$$

where

$$q_w=-k\frac{\partial T}{\partial y},\ q_m=-D_B\frac{\partial C}{\partial y},\ \tau_w=\mu\frac{\partial u}{\partial y}, \quad \text{at } y=0.$$

The associated expressions of dimensionless reduced Nusselt number $-\theta'(0)$, reduced Sherwood number $-\phi'(0)$ and skin-friction coefficient $C_{fx}(0)$ are defined as:

$$-\theta'(0)=\frac{Nu}{\sqrt{\frac{m+1}{2}\mathrm{Re}_x}},\ -\phi'(0)=\frac{Sh}{\sqrt{\frac{m+1}{2}\mathrm{Re}_x}},\ C_{fx}(0)=\frac{C_f}{2}\sqrt{\frac{2}{m+1}\mathrm{Re}_x}. \tag{12}$$

where $\mathrm{Re}_x=\frac{u_w(x)x}{\nu}$ is the local Reynolds number based on the stretching velocity. The transformed nonlinear ordinary differential Eqs. (8)-(10) subjected to boundary conditions (11) are solved numerically by means of Keller-box method [21-22].

RESULTS AND DISCUSSION

The stagnation-point flow of Nanofluids towards a nonlinear stretching sheet is theoretically studied. Numerical solutions are obtained using Keller-box method and the results are shown in various tables and figures for some physical parameters of interest. Table 1, shows a comparison of our results for reduced Nusselt number $-\theta'(0)$ and reduced Sherwood number $-\phi'(0)$ by taking the stretching parameter ε equal to zero and the power law velocity parameter $m = 1$ with those obtained by Khan and Pop [6]. This comparison shows an excellent agreement for the involved flow parameters. Hence we are quite confident that our results are accurate.

The variations of reduced Nusselt number $-\theta'(0)$, reduced Sherwood number $-\phi'(0)$ and skin-friction coefficient $C_{fx}(0)$ for different values of *Nb*, *Nt*, Pr, *Le*, ε and *m* are shown in Table 2, for the case of $\varepsilon < 1$. It is observed that $-\theta'(0)$ is a decreasing function of *Nb*, *Nt*, *Le* and *m* and an increasing one with respect to Pr and ε. However, it is found that $-\phi'(0)$ decreases for large values of *Nt*, Pr and *m* and increases for the increasing values of *Nb*, *Le* and ε. Further, it is observed that $C_{fx}(0)$ increases for the increasing values of *m* and decreases for the increasing values of ε. Table 3, presents results for the case $\varepsilon > 1$. It is found that the reduced Nusselt number $-\theta'(0)$ decreases for the increasing values of *Nb*, *Nt* and *Le* and increases for the increasing values of Pr, ε and *m*. The reduced Sherwood number $-\phi'(0)$ increases for the increasing values of *Nb*, *Nt*, *Le*, ε and *m* but decreases for the increasing values of Pr. Also, the skin-friction coefficient $C_{fx}(0)$ decreases as the values of ε and *m* are increased. Physically, it is true due to the fact that large values of Brownian motion parameter impacts a large extent of the fluid and results in thickening of the thermal boundary layer. Furthermore, the increasing values of thermophoresis parameter results in a deeper penetration into the fluid and causes the thermal boundary layer to be thicker.

Graphical results for different flow parameters are shown in Figures 1-13. The convergence of dimensionless velocity profiles for fixed values of *Nb*, *Nt*, Pr and *Le* is shown in Figure 1. This figure is plotted for velocity profiles to check the effects of *m* on the nanofluid motion for the both cases of $\varepsilon < 1$ and $\varepsilon > 1$. It is evident from this figure that when $\varepsilon < 1$, velocity profiles decrease for the increasing values of *m* whereas increase for increasing values of *m* when $\varepsilon > 1$. However, it is further observed that velocity profiles increase for increasing values of

Table 1: Comparison of the reduced Nusselt number $-\theta'(0)$ and the reduced Sherwood number $-\phi'(0)$ when $\varepsilon = 0$, Pr = *Le* = 10 and *m* = 1.

		Khan and Pop [6]		Present results	
Nb	Nt	θ'(0)	ϕ'(0)	θ'(0)	ϕ'(0)
0.1	0.1	0.9524	2.1294	0.9524	2.1294
0.2	0.2	0.3654	2.5152	0.3654	2.5152
0.3	0.3	0.1355	2.6088	0.1355	2.6088
0.4	0.4	0.0495	2.6038	0.0495	2.6038
0.5	0.5	0.0179	2.5731	0.0179	2.5731

Table 2: Variations of the reduced Nusselt number -θ'(0), the reduced Sherwood number -ϕ'(0) and skin-friction coefficient $C_{fx}(0)$ when ε < 1.

Nb	Nt	Pr	Le	ε	m	-θ?'(0)	-ϕ'(0)	$C_{fx}(0)$
0.1	0.1	1.0	10	0.1	0.5	0.5403	2.1956	0.8566
2.5	0.1	1.0	10	0.1	0.5	0.0626	2.3437	0.8566
0.1	2.0	1.0	10	0.1	0.5	0.2549	1.9469	0.8566
0.1	0.1	7.0	10	0.1	0.5	0.9834	2.1105	0.8566
0.1	0.1	1.0	25	0.1	0.5	0.5359	3.7205	0.8566
0.1	0.1	1.0	10	0.6	0.5	0.6335	2.2959	0.4830
0.1	0.1	1.0	10	0.1	5.0	0.5097	2.1396	1.1659

Table 3: Variations of the reduced Nusselt number -θ'(0), the reduced Sherwood number -ϕ'(0) and skin-friction coefficient $C_{fx}(0)$ when ε > 1.

Nb	Nt	Pr	Le	ε	m	-θ'(0)	-ϕ'(0)	$C_{fx}(0)$
0.1	0.1	1.0	10	1.1	0.5	0.7189	2.4219	-0.1415
2.5	0.1	1.0	10	1.1	0.5	0.0882	2.5595	-0.1415
0.1	2.0	1.0	10	1.1	0.5	0.3395	3.3578	-0.1415
0.1	0.1	7.0	10	1.1	0.5	1.0875	2.4113	-0.1415
0.1	0.1	1.0	25	1.1	0.5	0.7128	3.9473	-0.1415
0.1	0.1	1.0	10	2.0	0.5	0.8533	2.6608	-1.7255
0.1	0.1	1.0	10	0.1	5.0	0.7216	2.4293	-0.2026

ε for both cases $\varepsilon < 1$ and $\varepsilon > 1$. It is further noted that for $\varepsilon = 1$, the velocity profiles for different flow parameters coincide with each other. This means that in the case when the external stream velocity becomes equal to the stretching velocity, the flow field is not influenced by the different values of the incorporated parameters. This implies that the fluid velocity and surface velocity are same. It is interesting to note that for the case $\varepsilon > 1$, the external stream velocity increases compare to the stretching velocity and hence causes the shorten in thickness of the momentum boundary layer. However when $\varepsilon > 1$, it causes for the inverted boundary layer structure due to the fact that the stretching velocity of the surface exceeds the external stream velocity and results a decrease in the boundary layer thickness. It is worth mentioning that the dominance of free stream velocity is more effective to make shorten the momentum boundary layer thickness.

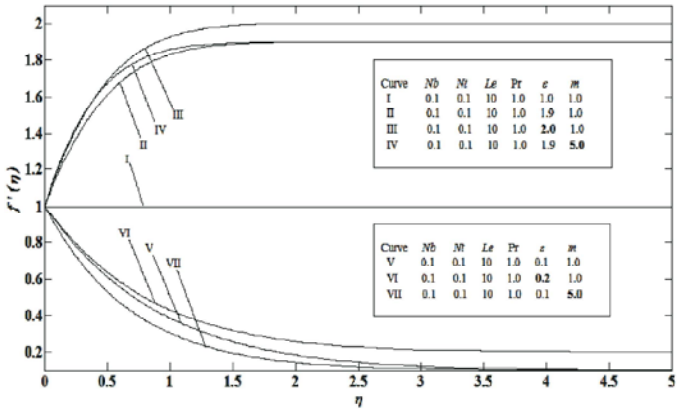

Fig. 1: Profiles of velocity for different values of $\varepsilon > 1$, $\varepsilon = 1$, $\varepsilon < 1$ and m

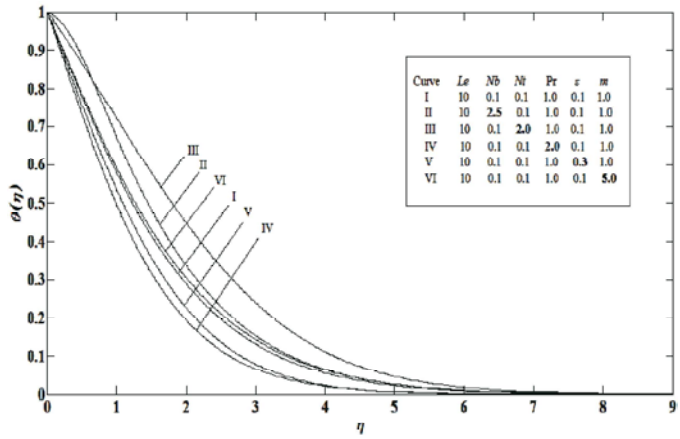

Fig. 2: Profiles of temperature for different values of Nb, Nt, Pr, $\varepsilon < 1$ and m

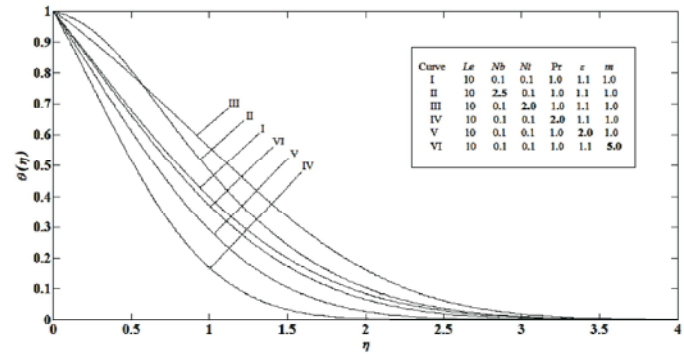

Fig. 3: Profiles of temperature for different values of Nb, Nt, Pr, $\varepsilon > 1$ and m

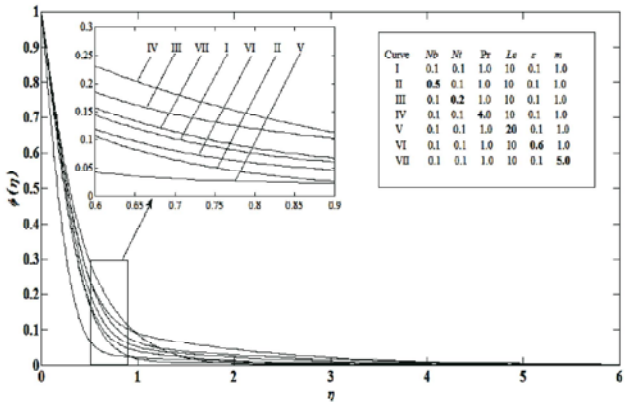

Fig. 4: Profiles of concentration for different values of *Nb*, *Nt*, Pr, *Le*, $\varepsilon < 1$ and *m*

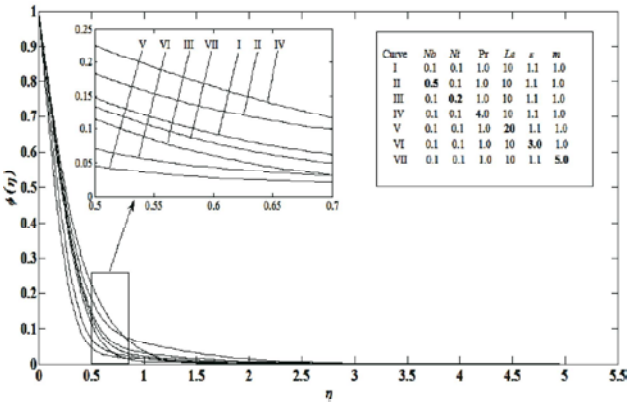

Fig. 5: Profiles of concentration for different values of *Nb*, *Nt*, Pr, *Le*, $\varepsilon > 1$ and *m*

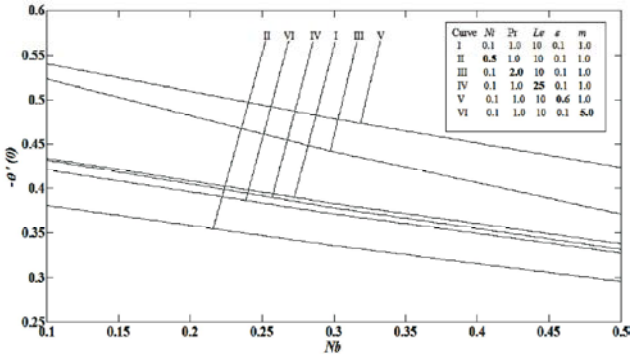

Fig. 6: Profiles of Nusselt number for different values of *Nt*, Pr, *Le*, $\varepsilon < 1$ and *m*

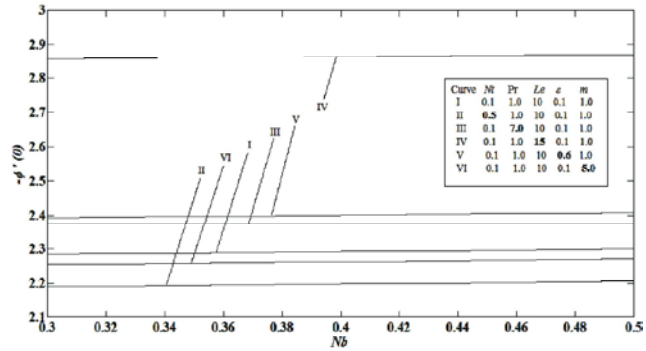

Fig. 7: Profiles of Sherwood number for different values of *Nt*, Pr, *Le*, $\varepsilon < 1$ and *m*

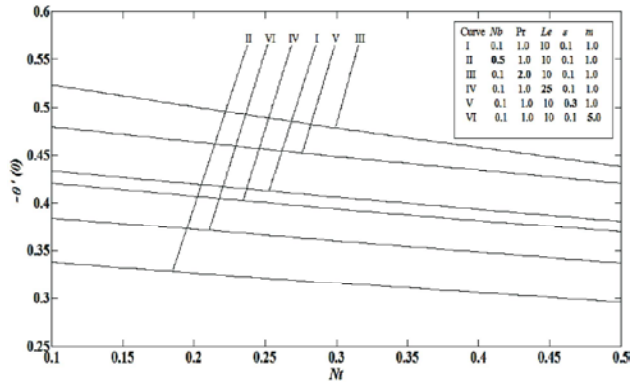

Fig. 8: Profiles of Nusselt number for different values of *Nb*, Pr, *Le*, $\varepsilon < 1$ and *m*

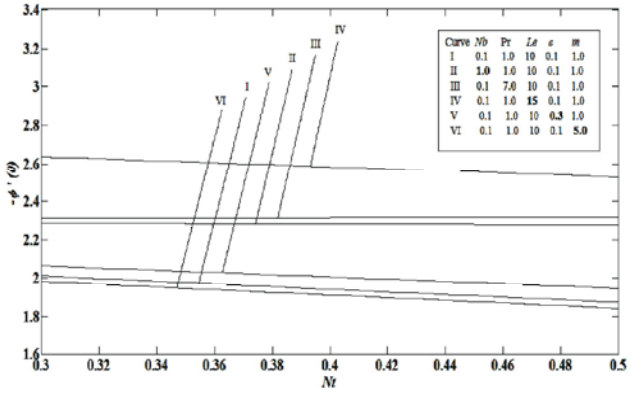

Fig. 9: Profiles of Sherwood number for different values of *Nt*, Pr, *Le*, $\varepsilon < 1$ and *m*

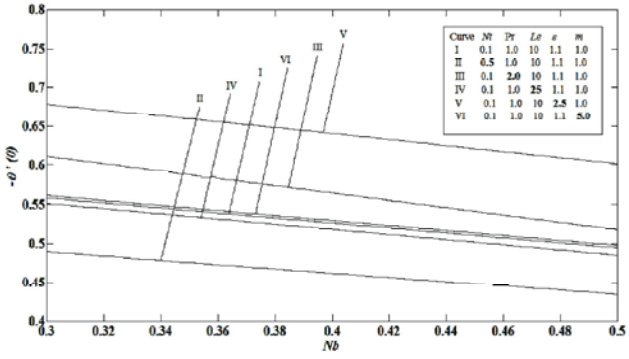

Fig. 10: Profiles of Nusselt number for different values of *Nt*, Pr, *Le*, $\varepsilon > 1$ and *m*

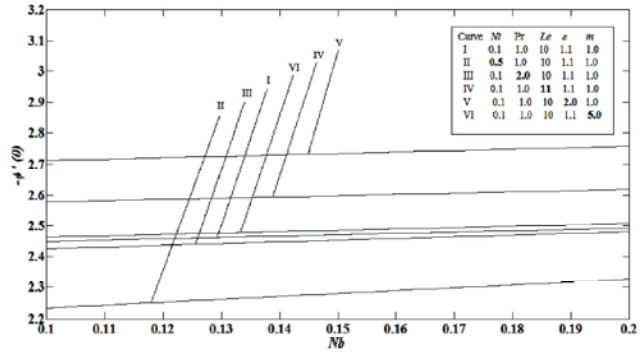

Fig. 11: Profiles of Sherwood number for different values of *Nt*, Pr, *Le*, $\varepsilon > 1$and *m*

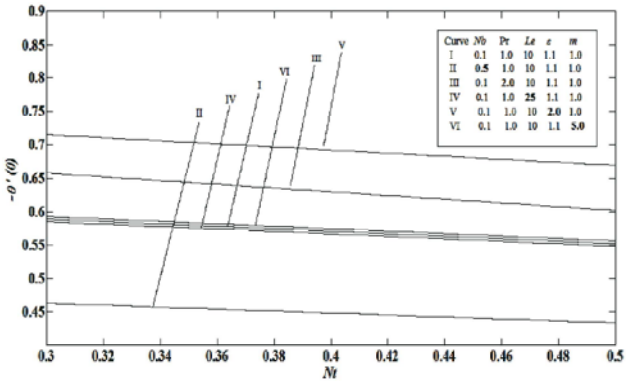

Fig. 12: Profiles of Nusselt number for different values of *Nb*, Pr, *Le*, $\varepsilon > 1$ and *m*

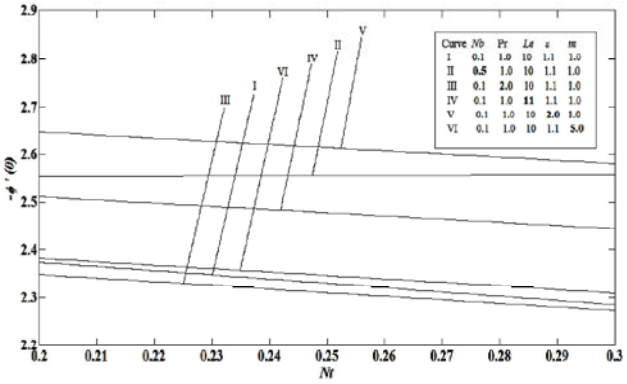

Fig. 13: Profiles of Sherwood number for different values of *Nb*, Pr, *Le*, $\varepsilon > 1$ and *m*

Figure 2, presents temperature profiles for the combined effects of *Nb*, *Nt*, Pr, *Le*, $\varepsilon < 1$ and *m*. It is observed that the increasing values of Pr and ε imply a decrease in the temperature whereas the temperature increases for increasing values of *Nb*, *Nt* and *m*. Physically, this behavior is meaningful due to the fact that it depends upon the formation of nanofluid which is a combination of the base fluid (water, ethylene glycol etc.) with nanoparticles (Cu, Aluminium, Titanium). With increasing viscosity of the base fluid, the thermal boundary layer thickness decreases and the heat transfer is found to be smaller for large values of Pr. Figure 3, is plotted for temperature profiles when $Le = 10$. This figure indicates that when external stream velocity is greater than the stretching velocity, the temperature profiles increase for increasing values of *Nb* and *Nt*. However it decreases for the increasing values of Pr, ε and *m*. This is due to the reason that nanofluid having high Prandtl number results with low thermal conductivities affecting the conduction phenomenon to shorten the thermal boundary layer thickness. The suspended nanoparticles motions are more affected by the highly viscous fluids and results in less colloidal forces among each other.

Figure 4, is prepared to study the effects of different incorporated flow parameters on concentration. It is depicted from this figure that increasing values of *Nb*, *Le* and $\varepsilon < 1$, causes a decrease in the mass transfer. However, the concentration increases for large values of *Nt*, Pr and *m*. Physically, it is meaningful that concentration decreases for large values of *Le* and play an important role in shortening the concentration boundary layer for the mass fraction. Since all profiles discussed above, descend smoothly in the free stream satisfying boundary conditions and ensure the accuracy of the obtained numerical results. Figure 5, depicts that for the dominated external stream velocity, concentration increases for increasing values of *Nb* and Pr whereas it decreases for increasing values of *Nt*, *Le*, $\varepsilon > 1$ and *m*. Furthermore, Figures 4 and 5 show that for $\varepsilon < 1$, the thermal boundary layer thickness and concentration boundary layer thickness are greater compare to the case $\varepsilon > 1$.

The variations of reduced Nusselt number $-\theta'(0)$, reduced Sherwood number $-\phi'(0)$ as functions of *Nb* for the different values of *Nt*, Pr, *Le*, $\varepsilon < 1$ and *m* are shown in Figures 6 and 7. From Figure 6, we observed that the

reduced Nusselt number increases for increasing values of Pr and ε and decreases for increasing values of *Nt*, *Le* and *m*. Further, it is observed from Figure 7, that the reduced Sherwood number decreases for increasing values of *Nt* and *m* while increases for increasing values of Pr, *Le* and ε. When $\varepsilon > 1$, Figures 8 and 9 elucidate the variation of the reduced Nusselt number and reduced Sherwood number along *Nt* for different values of the embedded flow parameters when external stream velocity is dominated by the stretching velocity. From Figure 8, it is found that the reduced Nusselt number decreases for increasing values of *Nb*, *Le* and *m* and increases for increasing values of Pr and ε. Figure 9, shows that the reduced Sherwood number increases for large values of *Nb*, Pr, *Le* and ε and decreases for increasing values of *m*.

For the case of $\varepsilon > 1$, Figures 10-13 present the variations of the reduced Nusselt number and reduced Sherwood number with *Nb* and *Nt*. Figure 10, shows that reduced Nusselt number decreases with increasing values of *Nt* and *Le* but it increases for increasing values of Pr, ε and *m*. Figure 11, shows that reduced Sherwood number increases for increasing values of *Le*, ε and *m* whereas decreases for the increasing values of *Nt* and Pr.

The variations of the reduced Nusselt number with *Nt* are given in Figure 12. This figure shows that reduced Nusselt number increases for increasing values of Pr, ε and *m*. and decreases for increasing values of *Nb* and *Le*. Finally, it is worth mentioning that in Figure 13, reduced Sherwood number along *Nt* increases with increasing values of *Nb*, *Le*, ε and *m*. It is found to be decreased as the values of Pr are increased.

CONCLUSION

Stagnation-point flow of nanofluid over a nonlinear stretching sheet is investigated. The model used here for nanofluid incorporates the effects of thermophoresis parameter *Nb*, Brownian motion *Nt*, Prandtl number Pr Lewis number *Le* velocity ratio parameter ε and nonlinear stretching parameter *m*. The governing nonlinear equations are numerically solved using implicit finite difference scheme known as Keller-box method. Numerical solutions depending upon all parameters are presented in tables and figures. For the accuracy purpose, we have compared our results with those of Khan and Pop [6]. An excellent agreement was noted.

ACKNOWLEDGEMENTS

The authors would like to acknowledge the financial support received from MOHE, Research Management Centre UTM University Teknologi Malaysia (4F109) and Universiti Malaysia Pahang (RDU110108).

REFERENCES

1. Kuznetsov, A.V. and D.A. Nield, 2010. Natural convective boundary-layer flow of a nanofluid past a vertical plate. Int. J. Therm. Sci., 49: 243-247.
2. Rana, P. and R. Bhargava, 2012. Flow and heat transfer of a nanofluid over a nonlinearly stretching sheet: A numerical study. Commun. Nonlinear Sci. Numer. Simul., 17: 212-226.
3. Bachok, N., A. Ishak and I. Pop, 2010. Boundary-layer flow of nanofluids over a moving surface in a flowing fluid. Int. J. Therm. Sci., 49: 1663-1668.
4. Anwar, M.I., S. Sharidan, I. Khan and M.Z. Salleh, 2012. Conjugate effects of radiation flux on double diffusive MHD free convection flow of a nanofluid over a power law stretching sheet. ISRN Thermodynamics, pp: 1-7.
5. Zheng, L., C. Zhang, X. Zhang and J. Zhang, 2013. Flow and radiation heat transfer of a nanofluid over a stretching sheet with velocity slip and temperature jump in porous medium. J. Franklin Institute., 350: 990-1007.
6. Khan, W.A. and I. Pop, 2010. Boundary-layer flow of a nanofluid past a stretching sheet. Int. J. Heat Mass Transf., 53: 2477-2483.
7. Anwar, M.I., I. Khan, S. Sharidan and M.Z. Salleh, 2012. Conjugate effects of heat and mass transfer of nanofluids over a nonlinear stretching sheet. Int. J. Phy. Sci., 7: 4081-4092.
8. Choi, S.U.S., 1995. Enhancing thermal conductivity of fluids with nanoparticles, Proceedings of the ASME International Mechanical Engineering Congress and Exposition, 231: 99-105. American Society of Mechanical Engineers, Fluids Engineering Division, San Francisco, Calif, USA.
9. Eastman, J.A., S.U.S. Choi, S. Li, W. Yu and L.J. Thompson, 2001. Anomalously increased effective thermal conductivity of ethylene glycol-based nanofluids containing copper nanoparticles. Appl. Phys. Lett., 78: 718-20.

10. Choi, S.U.S., Z.G. Zhang, W. Yu, F.E. Lockwood and E.A. Grulke, 2001. Anomalously thermal conductivity enhancement in nanotube suspensions. Appl. Phys. Lett., 79: 2252-4.
11. Masuda, H., A. Ebata, K. Teramae and N. Hishinuma, 1993. Alteration of thermal conductivity and viscosity of liquids by dispersing ultra-fine particles. Netsu Bussei., 7: 227-33.
12. Labropulu, F., D. Li and I. Pop, 2010. Non-orthogonal stagnation-point flow towards a stretching surface in a non-Newtonian fluid with heat transfer. Int. J. Therm. Sci., 49: 1042-1050.
13. Hiemenz, K., 1911. Die Grenzschicht an einem in den gleichformingen Flussigkeitsstrom eingetauchten graden Kreiszylinder. Dingler's Polytechnic Journal, 326: 321-324.
14. Nazar, R., N. Amin, D. Filip and I. Pop, 2004. Stagnation point flow of a micropolar fluid towards a stretching sheet. Int. J. Non-Linear Mech., 39: 1227-1235.
15. Lok, Y.Y., N. Amin and I. Pop, 2006. Non-orthogonal stagnation point flow towards a stretching sheet. Int. J. Non-Linear Mech., 41: 622-627.
16. Mahapatra, T.R. and A.S. Gupta, 2002. Heat transfer in stagnation-point flow towards a stretching sheet. Heat Mass Transf., 38: 517-521.
17. Mustafa, M., T. Hayat, I. Pop, S. Asghar and S. Obaidat, 2011. Stagnation-point flow of a nanofluid towards a stretching sheet. Int. J. Heat Mass Transf., 54: 5588-5594.
18. Hamad, M.A.A. and M. Ferdows, 2012. Similarity solution of boundary layer stagnation-point flow towards a heated porous stretching sheet saturated with a nanofluid with heat absorption/generation and suction/blowing: A lie group analysis. Commun. Nonlinear Sci. Numer. Simul., 17: 132-140.
19. Alsaedi, A., M. Awais and T. Hayat, 2012. Effects of heat generation/absorption on stagnation point flow of nanofluid over a surface with convective boundary conditions, Commun. Nonlinear Sci. Numer. Simul., http://dx.doi.org/10.1016/j.cnsns.2012.03.008. with "17, 4210 - 4223."
20. Afify, A.A., 2009. Similarity solution in MHD: Effects of thermal diffusion and diffusion thermo on free convective heat and mass transfer over a stretching surface considering suction or injection. Commun. Nonlinear Sci. Numer. Simul., 14: 2202-2214.
21. Cebeci, T. and P. Bradshaw, 1977. Momentum transfer in boundary layers. Hemisphere Publishing Corporation, New York.
22. Cebeci, T. and P. Bradshaw, 1988. Physical and computational aspects of convective heat transfer. Springer-Verlag, New York.